Heliyon 8 (2022) e10865

Contents lists available at ScienceDirect

Heliyon

journal homepage: www.cell.com/heliyon

Research article

Study of biomethanol as sustainable replacement of Autogas at variable ignition timing

Jayashish Kumar Pandey *, Dinesh M.H., Kumar G.N.

Department of Mechanical Engineering, National Institute of Technology Karnataka, Surathkal, Mangalore 575025, India

ARTICLE INFO

Keywords:
Bio-methanol
Autogas/LPG
Variable ignition timing
Combustion
CO/CO_2 emissions
NO_x emissions

ABSTRACT

Bio-methanol has recently interested researchers looking for a suitable alternative due to its low carbon/hydrogen (C/H) ratio. Adding methanol to Autogas could thereby improve combustion while lowering emissions. In the present investigation, testing is conducted at a compression ratio of 14:1 on various fuel ratios (55/45 to 75/25 with a 5% change) of methanol/Autogas with ignition timing ranging from 28°CA bTDC to 14°CA bTDC. The results indicate improvements due to the addition of 65% methanol. Improved brake thermal efficiency (BTE) by 6.27%, peak pressure (P_{max}) by 0.36%, heat release rate (HRR_{max}), peak temperature (T_{max}) by 0.89%, and rise in exhaust gas temperature (EGT). Simultaneously, combustion duration, HC & CO emissions, and the coefficient of variations in indicated mean effective pressure (CoV_{IMEP}) are reduced. With methanol, the volumetric efficiency (η_{vol}) improves continuously. Optimal ignition timing is shown to advance with increasing methanol concentration. With ignition retard, the flame development phase (CA10) decreases by 1.7%/2°CA ignition retard, whereas the flame propagation phase (CA10–90) decreases to a minimum and then increases. Due to combustion instability, ignition retard increases the Cyclic variation and CoV_{IMEP}, while P_{max}, HRR_{max}, T_{max}, and BTE increase to a maximum and then drop. Ignition retard is an effective way of reducing NO_x emissions, although CO and HC emissions increase significantly. Due to reduced carbon supply, carbon emissions are extremely low even at higher methanol concentrations than Autogas-rich fuel. NOx emissions are also extremely low (62.5 % of the ignition angle at 24°CA), revealing that a higher methanol ratio could be used with minimal risk of power loss.

1. Introduction

The transportation sector is experiencing a substantial dependence due to rising ease of life, flexible marketing, and rapid globalization. Hence, energy demands are increasing, putting more pressure on the rapidly depleting conventional energy sources. These conventional sources, which include gasoline, LPG, and diesel, are the primary cause of environmental degradation. Similar to gasoline, LPG is widely used as a transportation fuel known as Autogas. Over 17 million vehicles in Europe are powered by Autogas (reported in 2019 [1]), while in India, nearly a 2.4 million vehicles are powered by Autogas. Korea, Turkey, and Russia are the largest consumer of Autogas [2]. Autogas has certain benefits over gasoline; a higher heating value adds up extra energy to reduce specific energy consumption (SFC).

Similarly, it has a higher-octane number, which ensures knockproof operation. Higher laminar flame velocity helps better combustion, while higher autoignition temperature allows elevated CR operation, compensating for the drawbacks of low volumetric energy content. Autogas is a mixture of propane and butane. Hence, a simple chemical structure has less carbon content compared to gasoline. Hence, fewer carbon emissions are expected. According to the World LPG Association, the regulated emissions (CO, CO_2, HC, and NO_x) are less for Autogas than gasoline [1]. Even the PM emissions are less than gasoline under the new European driving cycle. However, compared to CNG-powered vehicles, emissions are very high for Autogas [3].

Nowadays, governments from various nations have expressed concern by implementing stringent norms, which legally limit automotive [4, 5, 6, 7]. Autogas is also a conventional hydrocarbon fuel; hence, concerns are raised. It is too a significant source of CO_2 emissions and is simultaneously perishable. Therefore, researchers have proposed replacing conventional fuel with sustainable, environmentally friendly, renewable fuel to meet these challenges. It should be bio-produced to stand with these multiple fuel criteria [8]. Among all the available options, such as hydrogen, biomass-oriented methane, bio-methanol, and bioethanol, bio-methanol has gained much interest from researchers [9]. Like synthetic methanol, bio-methanol remains in the liquid state at

* Corresponding author.
E-mail address: pandeyjayashish@gmail.com (J.K. Pandey).

https://doi.org/10.1016/j.heliyon.2022.e10865
Received 16 July 2022; Received in revised form 17 August 2022; Accepted 27 September 2022

standard conditions, helping transportation. However, bio-methanol production can be achieved through renewable sources like biowastes and woods [10]. Hence, governments in developing countries like India and Brazil motivate production [11, 12].

The fuel properties of bio-methanol are similar to synthetic, mainly depending on the presence of water content. 99% pure methanol has fuel properties prominent to IC engines without hefty modifications. It has 50% oxygen content, which reduces stoichiometric air demand [13]. Methanol possesses a high-octane number (Table 1) suitable for SI engines and provides efficient knock resistivity even at high CR. A wide flammability limit is helpful, but a lower flammability limit restricts ultra-lean operation [14]. A high hydrogen-to-carbon ratio and a single molecule structure limit the specific carbon emission [15]. Nathan Prasad and Kumar [16] showed a significant reduction in net carbon emission for 50% methanol blending, and a proper ignition led to a considerable reduction in NO_x emissions. However, Mishra et al. [17] had a slightly different analysis; they observed a slight increase in CO_2 emissions despite less CO, HC, and NO_x. They referred to increased SFC as the primary cause. In a similar study, Wang et al. [18] had reported a reduction in brake-specific NO_x and HC by increasing methanol in CNG. Elfasakhany [19], in his comparative study, notified that 10% methanol blending gasoline has nearly 55% and 26% reductions in CO and HC, respectively, while CO_2 is increased by 12%. He also pointed out improved performance by the M10 blend. In another study, Elfasakhany [20] studied blends of bio-methanol with butanol, CO and HC were reduced by increasing bio-methanol. However, performance slightly deteriorated. However, CO_2, though reduced below gasoline, it increased with bio-methanol fractions.

Though a bunch of research supports methanol as a sustainable fuel, Çelik et al. [21] has pointed out the issues with pure methanol; he emphasized changing CR for methanol as the brake thermal efficiency (BTE) is improved due to efficient combustion. They reported a reduction in CO and HC by increasing CR. Li et al. [22] specified that low vapor pressure and high latent heat are responsible for cold start problems, creating difficulties igniting under cold conditions and limiting the chances of methanol being used solely in the SI engine. Abu-Zaid et al. [23] had pointed out the upper limit of methanol addition to 15% for better performance. Similarly, Bilgin and Sezer [24] reported a loss in brake mean effective pressure (BMEP) and BTE after 15% methanol addition. They observed the excess latent heat responsible for cooling the engine and suggested increasing CR and carefully selecting ignition timing. However, Gong et al. [25] observed that the cold start problem is eliminated for methanol fuelling of Autogas engine even at low gas fractions (10%) at elevated CR. Balki and Sayin [26] noticed a higher CR operation of Autogas/Methanol blends reduces HC and CO, while NO_x and CO_2 are increased slightly. They reported that BTE, P_{max}, and heat release rate (HRR) increased to CR 9:1.

High CR has multiple benefits for high latent heat fuels [27]. It increases the MGT, cylinder wall, and manifold temperature, which diminishes the cold start issues of methanol due to high latent heat [28]. It improves engine breathing by reducing pumping loss, increasing volumetric efficiency, and improving power output and thermal efficiency [29]. Ravi et al. [30] experimentally verified reduction of CO emissions by nearly 33% by increasing CR to 10.5:1 from 9:1, while CA10 is also reduced and HRR and P_{max} are increased. Similarly, H. Chen et al. [31] had reported ignition delay is reduced and P_{max} and T_{max}, which helps achieve near-constant volume combustion. Elevated CR for LPG/methanol reduces formaldehyde and HC emissions caused by inconsistent combustion of methanol, while NO_x emissions are increased, but the lean limit improves.

Autogas has a higher autoignition temperature than methanol, supports high CR, and improves engine performance. Somasundaram et al. [33] had experimented with feeding methanol to an Autogas engine, observed increased mechanical efficiency, and reduced CO, CO_2, HC, and NO_x emissions at higher loads. Patil et al. [34] had studied a higher range of water-methanol addition to Autogas engine, they observed BTE increase up to 30% methanol up to 3000 rpm. At high load and speed, BTE is reduced with methanol. CO, CO_2, HC, and NO_x are reduced due to low T_{max}. The cold start firing was studied by Gong et al. [35], who concluded an early pickup for LPG/methanol compared to gasoline. Formaldehyde emissions are also reduced, and firing gets stabilized rapidly. However, Gong et al. [36] extensively studied the injection strategy and observed that P_{max} and maximum transient engine speed are increased by injecting a large amount of methanol/LPG per cycle. They pointed out that the injection strategy plays a vital role in HC and formaldehyde emissions; 74.4% reduced HC was observed for critical firing than misfiring. Ceviz et al. [37] analyzed the cyclic behavior and observed reducing cyclic variations at relatively lean fuelling. The combustion characteristics improve, increasing P_{max} and reducing carbon emissions. Hence, methanol could be considered a suitable replacement for Autogas.

Autogas and methanol have higher autoignition temperatures than gasoline, which increases CR. Javaheri et al. [38] concluded that the increasing CR reduces the ignition delay and increases the laminar flame velocity, resulting in fast combustion and higher cylinder pressure and HRR [38]. Priyadarsini et al. [39] noticed that low volumetric displacement causes an inefficient power conversion process in gaseous fuel; hence, increasing CR may improve the exhaust process and enhance volumetric efficiency (η_{vol}) [39]. Gong et al. [40] noticed that though the high latent heat fuel cools instream air to increase intake, vaporization is delayed, which elongates the combustion process. Abdel-Rahman and Osman [41] suggested that increasing CR would supply extra energy required in such cases for vaporization and sensible fuel heating due to increased MGT [41]. Zheng et al. [42] studied cyclic variation under variable CR and concluded that the combustion instability reduces, reducing the CoV_{IMEP} and cycle-by-cycle variations.

The CoV_{IMEP} also depends mainly on the ignition timing. Binjuwair and Alkudsi [43] observed that a much-advanced ignition has low pressure and temperature at the time of spark, which elongates the combustion and, in the course of compression, the combustion speed changes, resulting in increased CoV_{IMEP}. Similarly, emissions are also ignition dependent; Pandey and Kumar [44] pointed out that a delayed ignition for rapid burning fuel blends reduces combustion duration, CO, HC, and NO_x emissions. However, CO_2 emissions are increased slightly. Nevertheless, an excessively delayed ignition has adverse effects [45]. Gao et al. [46] point out that advancing ignition results in a continuous increase in cylinder pressure due to increased strength of compression of a relatively large mass burnt, increasing HRR due to increased fuel burning rate. However, the heat released during compression increases the negative compression work, which reduces BP. Tang et al. [47] reported increased NO_x and CO_2 by advancing ignition; BTE improved to a maximum.

Table 1. Properties of fuel [32].

Properties	Gasoline	Methanol	LPG
Chemical formula	Various	CH_3OH	$xC_3H_8 + (1 - x)\ C_4H_{10}$
Molecular weight (kg/kmol)	107	32.04	44
Oxygen Content by mass (%)	0	49.93	0
Hydrogen Content by mass (%)	~14	12.58	18.2
Carbon Content by mass (%)	~86	37.48	81.8
Lower heating value (MJ/kg)	42.90	20.09	46.4
Flammability limits (vol)	1.47–7.6	6.7–36	2.15–9.6
Research Octane Number (RON)	80–98	108.7	109.2
Motor Octane Number (MON)	81–84	88.6	89
Volumetric Energy Content (MJ/m^3)	31746	15871	24446
Stoichiometric AFR (kg/kg)	14.70	6.5	15.7
Autoignition temperature (K)	553	738	728
Adiabatic Flame Temperature(K)	~2275	2143	2250
Quenching distance (mm)	2.0–3.0	1.85	1.68–1.8
Laminar flame velocity (mm/s)	425	500	455
Minimum Ignition Energy (MIE)	0.8	0.14	0.26

On the other hand, Prasad et al. [48] have favored delayed ignition for gaseous fuel, which increases thermal conditions at the time of spark, reducing the CA10 but CA10–90 after achieving a minimum increase. It reduces T_{max}, which reduces NO_x emissions; however, further delay in ignition increases carbon emissions after a certain ignition angle. Hence, they suggested that selection of optimum ignition timing an essential.

Therefore, for a two-phase binary fuel Autogas/Methanol, the selection of an optimal ignition timing is needed. It has also been noticed through practical studies that the ignition timing for such two-phase binary fuel varies with a range of speed [49]. Second, the emissions are also largely dependent on the ignition, which too directs in the same way.

Research the advantages of methanol/Autogas as an internal combustion engine fuel. Few academics have conducted extensive research on the topic. Due to its low carbon structure and characteristics, methanol/Autogas has recently become more popular as a fuel. To establish a carbon-free or carbon-reduced economy in the 21st century without affecting IC engine efficiency, the research community must investigate, encourage, and expand research on methanol/Autogas as an internal combustion engine fuel. The use of methanol/Autogas fuels in SI engines would likely be sustainable. Even though the researchers have not investigated the variables with which we can work, our investigation gave substantial insight into the planning of variable-characteristic methanol/Autogas-fuelled SI engines. Therefore, in the current studies, an experimental investigation is conducted for various fractions of methanol at various ignition timings.

2. Experimental set-up and procedure

2.1. Experimental set-up

All the experiments are performed on a single-cylinder four-stroke variable compression ratio (hydraulically liftable cylinder block) SI engine. The specifications of the engine are listed in Table 2.

A small hole is drilled towards the combustion chamber to install the piezo senor (PCB Piezotronics, Model SM111A22). The throttle body is fitted with a MAP sensor. A PFI fuel pump and an injector are installed in the intake manifold after the throttle body for methanol. Another port injector for Autogas gas is installed parallel to the PFI injectors. Similarly, the exhaust manifold is fitted with a K-type thermocouple at 180 mm from the exhaust valve to measure the exhaust gas temperature at the manifold. The tailpipe is connected with a shell and tube-type calorimeter with a single exhaust gas pass. An eddy current dynamometer (Make-Technomech, Model- TMEC10) is coupled with the crankshaft and is fitted with a crank encoder. A spur gear type 360° précised disc with a trigger mark is installed on the crankshaft, which reads the crank angles by a photoelectric cell. The sensor data is sent to the engine management system.

The gas fuel line was consisting a 19.2 kg capacity gas cylinder filled with auto-fuel LPG/Autogas, which has a composition of 80% propane and 20% butane. The fuel line is connected to a wet-type flame arrestor fitted with a pressure gauge (0–10 bar) and a safety valve (Make-ELGI equipment, A020002, 3/8 Inch, 1–7 bar). Further, an Autogas flow meter with a flow control valve (Make-ATN, 0-10LPM, least count 0.01LPM) is connected, followed by an electronic sequential pressure regulator (Make- Auto Fuels, 1.2 bar–3 bar output). The gas ECU governs the electronically controlled Autogas injector (Make-AutoGas AC STAG 300), following the injection timing commands from the reprogrammable ECU (Make-Performance Electronics, PE3-8400) installed for controlling the methanol injector. All the sensor data are synchronized to a LabView-based program for parametric analysis through a data acquisition system (16-bit DAQ, NI-USB-6210). The specifications of the measurement devices installed are provided in Table 3, and the schematic diagram of the test set-up is shown in Figure 1a. The exhaust gas emissions are measured with the help of a five-gas analyzer (Make: Indus Scientific Pvt. Ltd., PEA250N) (see Figure 1b).

Table 2. Engine specifications.

Model	Kirloskar TV1, water-cooled
Bore	87.5 mm
Stroke	110 mm
Piston bowl geometry	Hemispherical (Ø52 mm)
CR	Variable (08:1–15:1, 14:1 for experiments)
No. of cylinders	1
Top speed	1800 rpm
Ignition timing	Variable
Dynamometer	Water-cooled Eddy current type
Crank angle sensor	Resolution 1°, Speed 5500 rpm with TDC pulse
Data acquisition device	NI USB-6210, 16-bit, 250 kS/s
Electronic control Unit	PE3-8400

2.2. Methodology

All the experiments are performed under wide-open throttle conditions, keeping the CR fixed at 14. The selection is based upon a trade-off between different characteristics, such as BTE, η_{vol}, and emissions, experienced in our previous research [32]. The methanol energy fraction varies from 55% to 75% at a 5% interval based on the energy supplied by gasoline at CR11 and 24°CA bTDC. The injector opening duration is set accordingly. The ignition timing varies from 28°CA bTDC to 14°CA bTDC, at an interval of 2°CA at 1800rpm. Each experiment is repeated twice to minimize the errors. Each set of experiments uses 100 cycles for sampling. Based on average, the analysis is done with the help of the LabVIEW-based program. The emission data have chosen to get at least 2 min of reading with the operating software provided with the devices. The average data collection is considered for all three experiments under repeat. Since the exhaust gas analyzer provides output in parts per million (ppm) for HC and NO_x and % of vol. for CO and CO_2, which is converted to g/kWh by using Eqs. (1) and (2) on a dry basis [50].

$$SE_i = VE_i\left\{\frac{M_i}{M_{ex}} \times \frac{\dot{m}_{ex}}{BP}\right\} \tag{1}$$

$$\dot{m}_{ex} = mass\ flow\ rate\ of\ exhaust = \dot{m}_f + \dot{m}_{air} \tag{2}$$

Table 3. Specifications of measuring equipment.

Equipment	Specification
K-Type Thermocouple	Thermocouple grade wire (270 °C to 1260 °C)
	Standard: ±2.2 °C or ±0.75%
RTD Temperature Sensors	PT100 Series, Sensing Element: Single 100-U platinum (Pt 100), 3-wire; TCR = 0.00385 Ω/°C
	Probe: 6 mm, 316 stainless steel sheath, single RTD is embedded in alumina powder
	Sensitivity: class A ± [0.15 + 0.002 |t|] °C, 5 s response time
	Range: 0 °C–1150 °C
Airflow measurement transmitter	Accuracy ≤0.25 (BFSL) % of span
	Response time (10–90%) ≤ 1 ms
Load cell	Zero balance (FSO) ±0.1 mV/V
	Tolerance on output (FSO) ±0.25%
	Non-linearity (FSO) <±0.025%
Piezo-sensor	Rise time – 2 ms
	Sensitivity – 1 mV/psi
	Resolution – 0.1 psi
	Resonant frequency – 400 kHz
	Low frequency response (5%) – 0.001 Hz
	Discharge time constant – 500 s

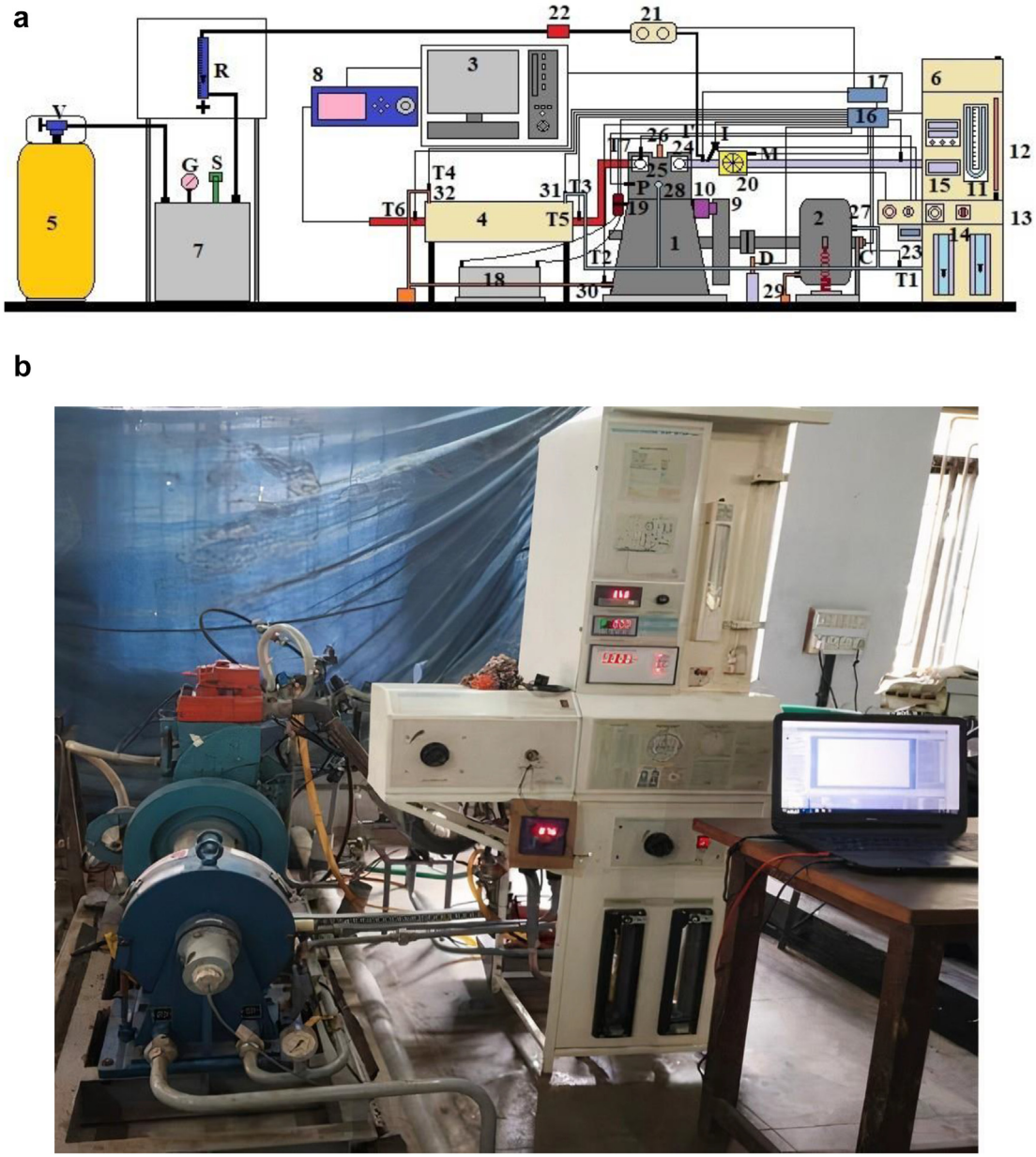

Figure 1. (a) Schematic of the test set-up.1-Engine, 2-Dynamometer, 3-Computer, 4-Calorimeter, 5- Autogas -Cylinder, 6-Fuel tank, 7-Wet flame arrester, 8-Exhaust gas analyzer, 9-Flywheel, 10-Starter motor, 11-Manometer, 12-Fuel burette, 13-Air-box, 14-Water rotameters, 15-Load knob, 16-Open ECU (primary), 17-Gas ECU, 18-Battery, 19-Capacitor, 20-Throttle-body, 21-Sequential reducer, 22-Dry flame trap, 23-T7 display, 24-Inlet-manifold, 25-Exhaust manifold, 26-Spark-plug, 27-Water inlet (dynamometer), 28-Water inlet (engine), 29-Water outlet (dynamometer), 30-Water outlet (engine), 31-Water inlet (calorimeter), 32-Water outlet (calorimeter), C-Crank encoder, D-Crank Position Sensor, G-Pressure gauge, M-MAP Sensor, P-Pressure Transducer, R-Gas rotameter, S-Safety valve, T1-Thermocouple (inlet water, engine & dynamometer), T2-Thermocouple (outlet water, engine), T3-Thermocouple (inlet water, calorimeter), T4-Thermocouple (outlet water, calorimeter), T5-Thermocouple (exhaust gas inlet, calorimeter), T6-Thermocouple (exhaust gas outlet, calorimeter), T7-Thermocouple (exhaust gas, manifold), V- Autogas Supply valve. (b) Experimental test-rig.

M_{ex} = molecular weight of exhaust, calculated on stoichiometric combustion = 28.72(gasoline) & 28.04(dual fuel)

SE_i = *Specific emission of any entity*

VE_i = *Emission data recorded by the analyzer of the entity*

M_i = *molecular weight of entity*

An excel program is developed to convert the volumetric emissions into specific emissions as the mass flow rate of exhaust varies with speed and volumetric efficiency.

1-Engine, 2-Dynamometer, 3-Computer, 4-Calorimeter, 5-Autogas-Cylinder, 6-Fuel tank, 7-Wet flame arrester, 8-Exhaust gas analyzer, 9-Flywheel, 10-Starter motor, 11-Manometer, 12-Fuel burette, 13-Air-box, 14-Water rotameters, 15-Load knob, 16-Open ECU (primary), 17-Gas ECU, 18-Battery, 19-Capacitor, 20-Throttle-body, 21-Sequential reducer, 22-Dry flame trap, 23-T_7 display, 24-Inlet-manifold, 25-Exhaust manifold, 26-Spark-plug, 27-Water inlet (dynamometer), 28-Water inlet

(engine), 29-Water outlet (dynamometer), 30-Water outlet (engine), 31-Water inlet (calorimeter), 32-Water outlet (calorimeter), C-Crank encoder, D-Crank Position Sensor, G-Pressure gauge, M-MAP Sensor, P-Pressure Transducer, R-Gas rotameter, S-Safety valve, T_1-Thermocouple (inlet water, engine & dynamometer), T_2-Thermocouple (outlet water, engine), T_3-Thermocouple (inlet water, calorimeter), T_4-Thermocouple (outlet water, calorimeter), T_5-Thermocouple (exhaust gas inlet, calorimeter), T6-Thermocouple (exhaust gas outlet, calorimeter), T7-Thermocouple (exhaust gas, manifold), V-Autogas Supply valve.

The error analysis is performed for the sample size by considering the standard deviations through the mean of the data collected from all the sensors and the calculated dependent variables such as BP, BTE, and BSEC by the equations mentioned in Ref. [51]. The uncertainty calculated throughout the experiments falls under the 1.4% range. However, the gas analyzer's % deviation ranges from 2.14% for CO to 4.32% for NO_x.

3. Results and discussion

All the experiments are conducted under similar conditions. The test results are grouped based on the two speeds for comparison. The findings are listed below according to the significant comparable parameters.

3.1. Brake thermal efficiency (BTE) and brake specific fuel consumption (BSFC)

Figure 2 shows an improvement in BTE with increasing methanol share up to 65%; however, the increment rate decreases after and drops continuously with ignition retard. The ignition retards observe an increment in BTE to an optimum and then worsen. Methanol fraction has a significant impact on the best ignition timing. An advanced ignition is good at a low methanol fraction, as, for 55M45L, 24°CA bTDC results better, while for 75M25L, 20°CA bTDC is good. Methanol owns high laminar flame velocity, resulting in fast combustion that improves BTE [29], while Autogas has slightly low flame speed, which delays combustion. Hence, the optimal ignition timing retards with increasing methanol strength.

On the other hand, though the high latent heat of methanol is responsible for cooling the working fluid and reducing compression work, which could improve BTE, it cools cylinder temperature that elongates the delay period. Hence, a large amount of mass burning falls in the expansion stroke [52]. Therefore, BTE reduces for methanol fractions above 65%; a delayed ignition helps overcome the latent effect [32]. The higher Autogas fraction reduces this benefit. Besides, the increasing Autogas also increases stratification, affecting power conversion and reducing the BTE [53]. For such Autogas-rich fuel, advanced ignition proves better. For 55M45L, BTE increases by 6.27%, at 24°CA bTDC from 14°CA bTDC. The reduction in Autogas fraction shifts the ignition timing corresponding to the optimum to a retarded position. Such the 24°CA bTDC ignition of 55M45L shifts to 20°CA bTDC for 75M25L at 1500 rpm.

3.2. Combustion durations

3.2.1. Flame development phase (CA10)

Figure 3, representing CA10, observes a reduction with increasing methanol fractions up to 65M35L. It observes an average 2.14% drop for 60M40L from 55M45L, which reduces to 0.94% for 65M35L. At low methanol share, Autogas dominates, reducing laminar flame velocity and increasing the stratification extent; hence, CA10 is higher [54]. However, after 65% methanol share, a further increase in methanol leads to a long ignition delay due to latent effects, increasing the CA10. CA10 increases by 1.13% on average per 5% increase in methanol share after 65M35L. CA10 reduces continuously with retarding the ignition. Probably the delayed ignition leads to higher cylinder temperature, increasing the flame velocity, which helps in quick flame stabilization [55]. There is an average 1.75% drop in CA10 for 75M25L with retarding ignition, increasing to 2.24% for 55M45L.

3.2.2. Flame propagation phase/rapid combustion zone (CA10–90)

Autogas/methanol blend ratio exhibits a similar effect on CA10–90 as CA10 (Figure 4). The increasing methanol share intends to reduce CA10–90; at 28°CA bTDC, there is a 2.14% reduction for 60M40L from 55M45L, which reduces to 0.58% for 65M35L. For low methanol fuel, CA10–90 increases due to reduced laminar flame speed. On the other hand, retarding ignition helps in increasing laminar speed and helps reduce CA10–90 to a minimum. Retarding the different ignition results in the completion of CA10 in the expansion stroke, leading CA10–90 to fall, where rapid pressure-drop reduces laminar flame speed and increases CA10–90. Also, a higher Autogas strength results in a lower overall flame speed, increasing the CA10–90 further. CA10–90 increases by 0.18%–2.83% from 24°CA bTDC to 14°CA bTDC at 75M25L, and by 0.36%–3.62% from 26°CA bTDC to 14°CA bTDC.

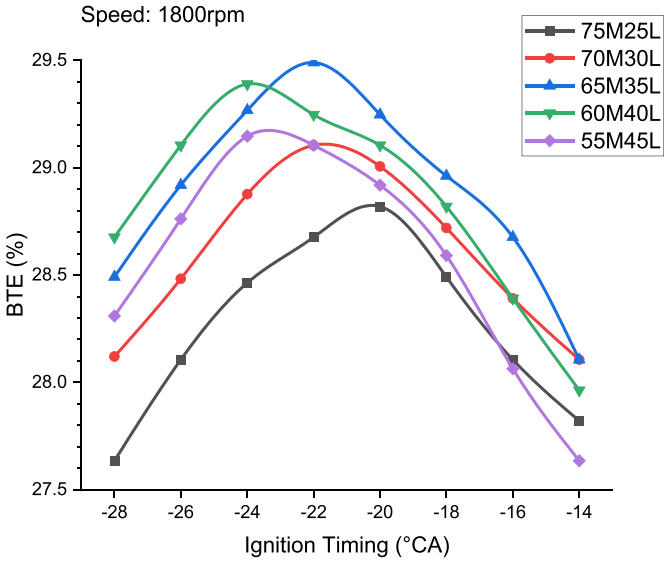

Figure 2. BTE variations with ignition timing at various Autogas fractions.

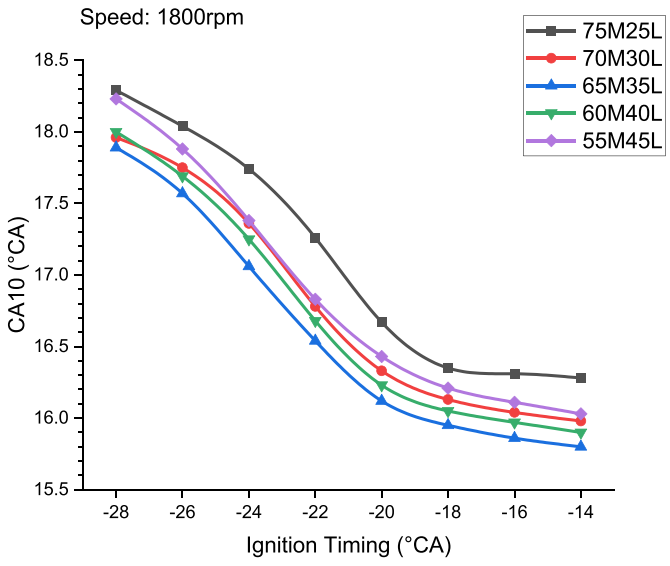

Figure 3. CA10 variations with ignition timing at various Autogas fractions.

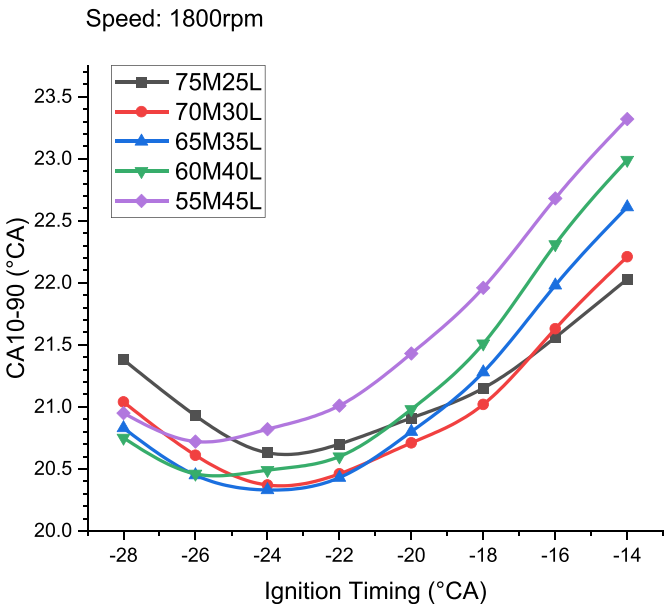

Figure 4. CA10–90 variations with ignition timing at various Autogas fractions.

3.3. Peak cylinder pressure (P_{max}) and position of peak cylinder pressure (θ/P_{max})

The energy supplied by the fuels is constant; therefore, the character of P_{max} depends solely on the quality of combustion, reflecting the impact of flame velocity and stratification. At lower Autogas fractions, the disadvantage of methanol, such as slow reaction due to high latent heat and small vapor pressure, is compensated by Autogas, which promotes rapid combustion. Besides, the stratification near the spark plug has a smaller zone of the richness of Autogas; hence flame stabilization gets quickly involved in rapid combustion [32], increasing and advancing P_{max}. However, high Autogas share reduces overall flame speed and increases the wideness of the richness zone, reducing combustion speed, resulting in reduced and retarded P_{max}. Referring to Figure 5, P_{max} increases with Autogas strength from 75M25L to 65M35L and then drops at all speeds. The increment rate reduces from 1.18% (75M25L to 70M30L) to 0.36% (70M30L to 65M35L) at 28°CA bTDC. Similarly, θ/P_{max} advances from 372°CA to 364°CA from 75M25L to 60M40L and then increases slightly at 28°CA bTDC. Retarding ignition at this stage helps improve P_{max} at high methanol share (up to 65M35L) but a retarded θ/P_{max}. There is an average 0.35%–0.13% increase in P_{max} by retarding ignition from 28°CA bTDC to 26°CA bTDC. A further retard in ignition results in a rapid drop in P_{max}, and θ/P_{max} retards at a higher rate. A similar outcome is persistent for low methanol share by retarding ignition from 28°CA bTDC. An average 11°CA shift of P_{max} at 75M25L increases to 18°CA at 55M45L. The reduction rate increases with increasing Autogas as well as retarding ignition. Since retarding ignition pushes a major part of combustion in the expansion stroke, it elongates the combustion duration and faces a rapid increase in cylinder volume; hence, P_{max} reduces [56].

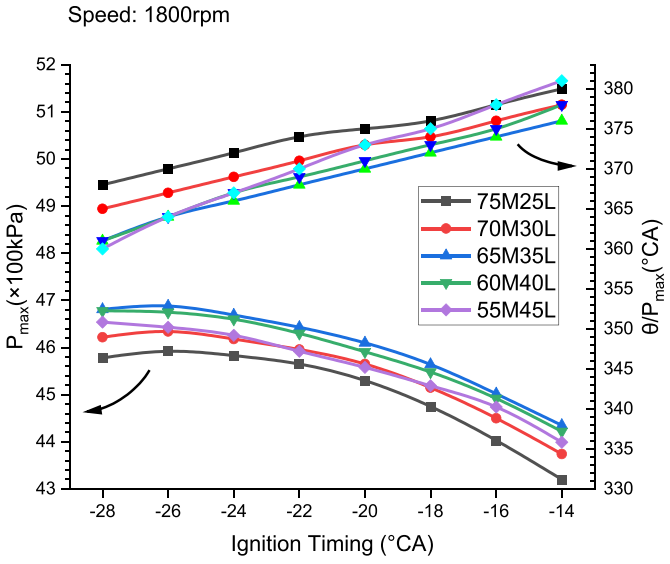

Figure 5. P_{max} and θ/P_{max} variations with ignition timing at various Autogas fractions.

3.4. Peak cylinder temperature (T_{max})

T_{max} follows P_{max} (referring to Figure 6); T_{max} witnesses a 2.13% reduction for 75M25L than 70M30L at 28°CA bTDC, which reduces to 0.89% for 65M35L than 60M40L. Since an early ignition faces cold conditions due to higher methanol, ignition lag elongates, leading to a lower rate of temperature rise, reducing the T_{max}. Therefore, a slight delay in ignition helps improve burning and increases T_{max}. An average 1.32% increase in T_{max} is noticed by retarding ignition to 26°CA bTDC from 28°CA bTDC for 75M25L to 65M35L. The increment rate of T_{max} reduces with the strength of Autogas, leading to reduce after Autogas increased above 35%. However, for all the blends, retarding ignition after 24°CA bTDC results in longer combustion duration due to the shift of the combustion zone, reducing the T_{max} continuously. The reduction rate increases with the extent of ignition retard. For the higher methanol, the reduction is much faster than Autogas-rich fuel, as, for 75M25L, an average reduction of 1.92%/2°CA ignition retard is noticed, which is 1.39%/2°CA ignition retard at 55M65L. Also, the ignition timing of optimal T_{max} shifts to a retarded position with methanol strength.

3.5. Cyclic variations in IMEP and coefficient of variations in IMEP (CoV_{IMEP})

3.5.1. Influence of blend ratio

Figure 7 represents cycle-by-cycle variations in IMEP for different Autogas/methanol fractions at 20°CA bTDC, considering 50 consecutive cycles. The increasing methanol fraction increases combustion speed and cools of instream air, which increases intake. Hence, combustion is regularised, and cycle-by-cycle variations are reduced. However, with a further increase in methanol, delayed ignition results in irregular

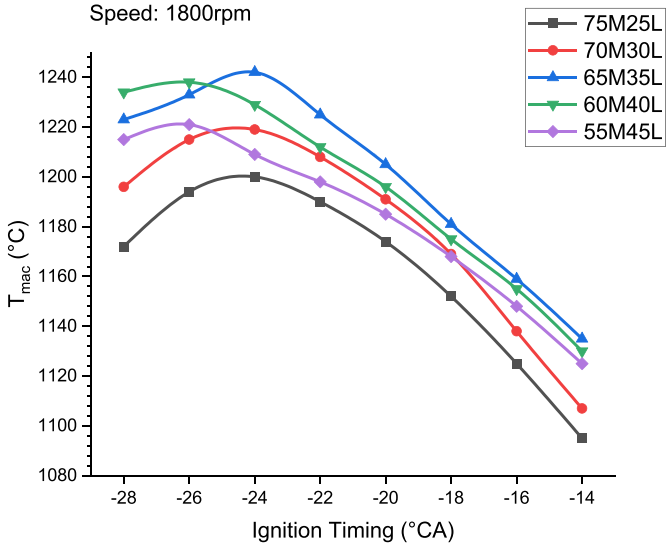

Figure 6. T_{max} variations with ignition timing at various Autogas fractions.

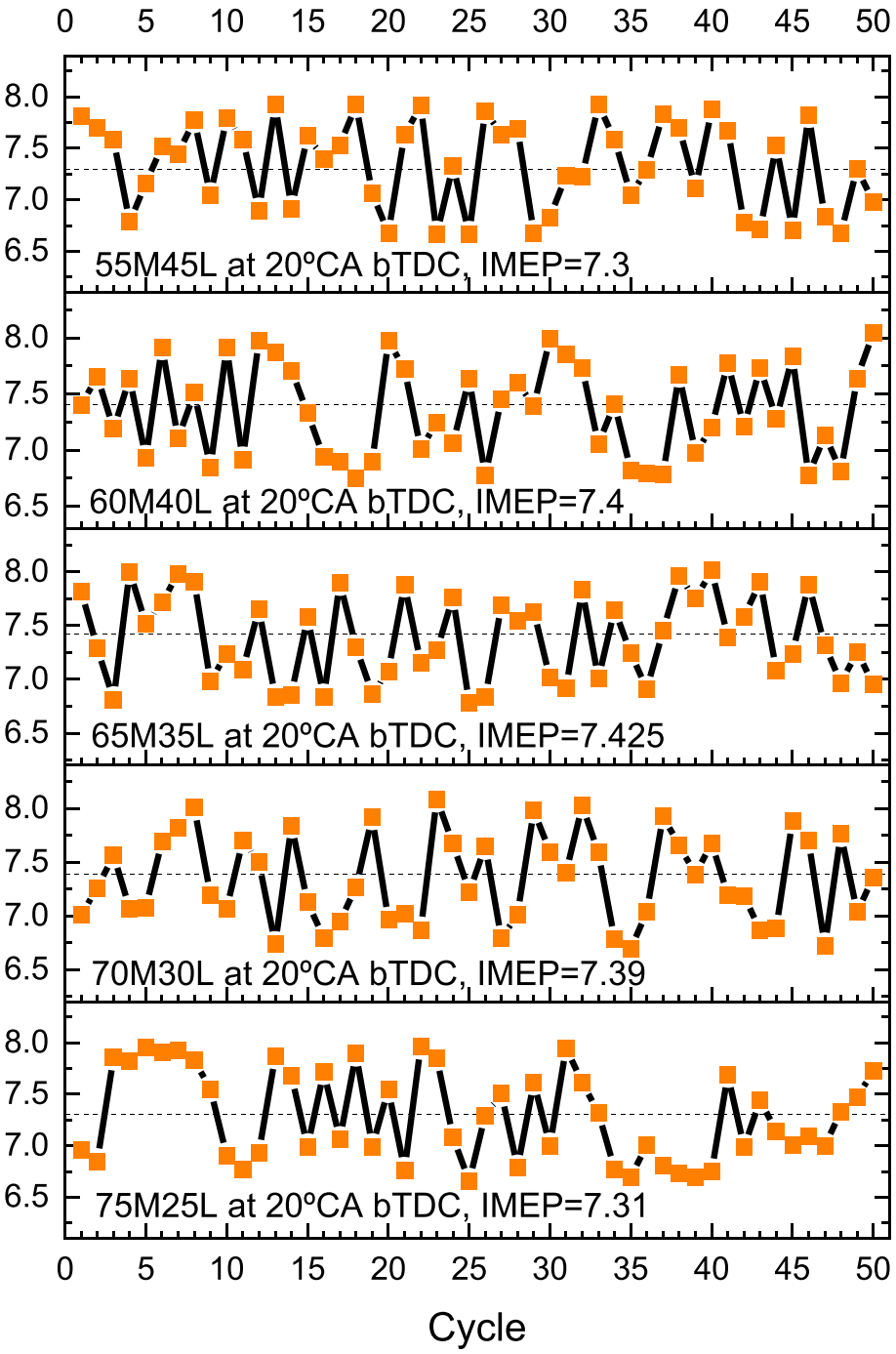

Figure 7. Cyclic variations at 20°CA bTDC at 1800 rpm.

combustion patterns leading to increase cycle-by-cycle variations. Figure 8 represents CoV_{IMEP}. The increasing blend strength of methanol reduces CoV_{IMEP}, as, for 60M40L, there is a 7.83% drop in CoV_{IMEP} from 55M45L at 28°CA bTDC, which reduces to 2.07% for 65M35L at the same ignition timing. However, a further increase in methanol increases it; at 70M30L, CoV_{IMEP} increases by 7.8%, while at 75M35L, it is increased by 6.1% at 28°CA bTDC. Due to the increased Autogas fraction, the reduction in η_{vol} reduces the turbulence intensity caused by tumble motion, and reduced laminar flame velocity also reduces the combustion speed. While, at higher methanol, the high latent heat reduces cylinder temperature, creating difficulties for the flame to sustain; therefore, cyclic variations increase.

3.5.2. *Influence of ignition timing*

Figure 9 represents cyclic variations against ignition timing for 65M35L. Ignition timing is one of the prime factors deciding combustion characteristics, such as speed and burning zones. A highly advanced ignition increases CA10 and CA100, leading to a slow flame stabilization, which reduces the turbulence motion. Hence, cyclic variability and CoV_{IMEP} are high (Figure 8). Retarding the ignition from 28°CA bTDC helps increase mixture temperature at the time of spark, leading to quickly developing flame. Hence, fast combustion reduces the cyclic variation. CoV_{IMEP} reduces from 1.38% at 28°CA bTDC to 1.13% at 22°CA bTDC for 55M45L; however, increasing methanol strength further reduces it mentioned in the above section. Hence, CoV_{IMEP} drops to

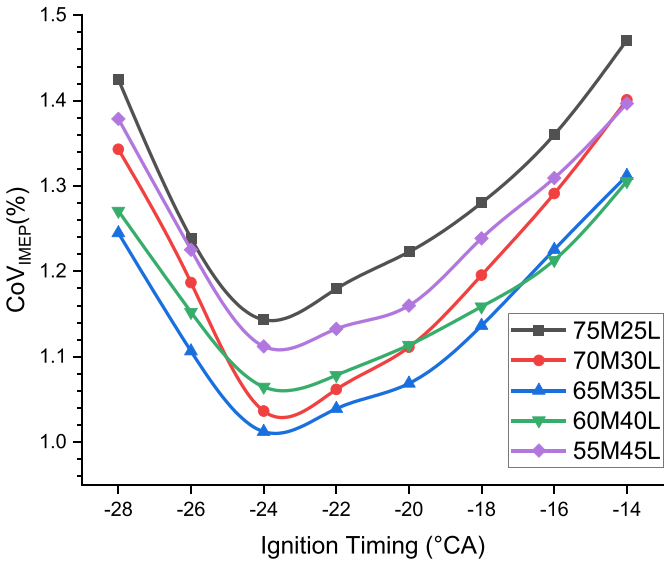

Figure 8. CoV_{IMEP} variations with ignition timing at various Autogas fractions.

1.24% at 28°CA bTDC and 1.03% at 22°CA bTDC for 65M35L. There is a small increment in CoV_{IMEP} after 65M35L due to increased combustion duration. Retarding ignition further compels a large part of mass burning in the expansion stroke, resulting in a significant drop in T_{max} and introducing combustion instabilities at a large scale. Therefore, the cyclic variations and CoV_{IMEP} increase.

3.6. Exhaust gas temperature (EGT)

Figure 10 shows EGT variations with ignition timing for various fuel combinations. EGT is a reference to perceive engine exhaust emissions and cylinder inner temperature. EGT is highly influenced by the strength of methanol, as the fast combustion characteristics of methanol lead to shortening combustion, allowing a small fraction of fuel to burn in expansion. Hence, EGT reduces. There is a 3.87% reduction in EGT at 28°CA bTDC for 70M30L, which is a further 2.3% for 60M40L. However, with increasing methanol, the probability of MGT-reduction increases, leading to elongated combustion resulting in an increased EGT at 75M25L (1.18% at 28°CA bTDC). While increasing Autogas strength also slows down combustion, leading to higher EGT, as for 55M45L, a 3.86% increment is noticed from 60M40L at 28°CA bTDC. However, the methanol effect increases with retarding ignition at higher methanol, as the average reduction rate at 60M40L is increased to 4.43% at 14°CA bTDC from 2.3% at 28°CA bTDC. At higher Autogas strength, the methanol effect is continuously reduced with retarding ignition, as at 60M40L reduction rate reduces from 3.86% at 28°CA bTDC to 1.82% at 14°CA bTDC.

3.7. Exhaust emissions

3.7.1. CO emissions

CO emissions arise primarily due to incomplete combustion. Since, at higher Autogas strength, the flame velocity is less, which delays combustion [32], forcing a larger mass of fuel to burn in the expansion stroke. Hence CO emissions increase due to the increased extent of incomplete combustion (Figure 11). An average 1.34% increase per 5% increase in Autogas was noticed at 28°CA bTDC. While methanol contribution is raised, it increases flame traveling speed and reduces quenching distance, assuring complete combustion of a larger mass. Also, indigenous oxygen increases that help efficient conversion of CO to CO_2. Therefore, CO emissions reduce with methanol. An average 4.14% drop/5% methanol increment was noticed at 28°CA bTDC up to 65M35L, while a 4.32% increment was noticed for 70M30L from 65M35L. However, it is still 4.06% less than 55M45L. Since increasing methanol cools the working fluid, it gradually elongates the delay period after a certain fraction, leading to incomplete combustion. Also, the leanness increases under WOT conditions with increasing methanol, which reduces flame speed. A 6.07% increment is noticed for 75M25L from 70M30L, and a 1.28% increase from 55M45L is noticed at 28°CA bTDC. However, ignition retard helps achieve better combustion for higher methanol fractions than 55M45L because the higher laminar flame speed and greater extent of compression overcome latent drawbacks of methanol. An average 6.81% drop/2°CA ignition retard is noticed for 75M25L from 55M45L. However, a retarded ignition shifts the combustion zone to a retarded position for any fuel blend. Hence, rapidly reducing pressure limits the complete burning of fuel, and CO emissions increase. The increment rate intensifies with ignition retard. For 75M25L, there is an average 3.23% increase in CO at 26°CA bTDC from 28°CA bTDC, which increases to 7.38% at 14°CA bTDC.

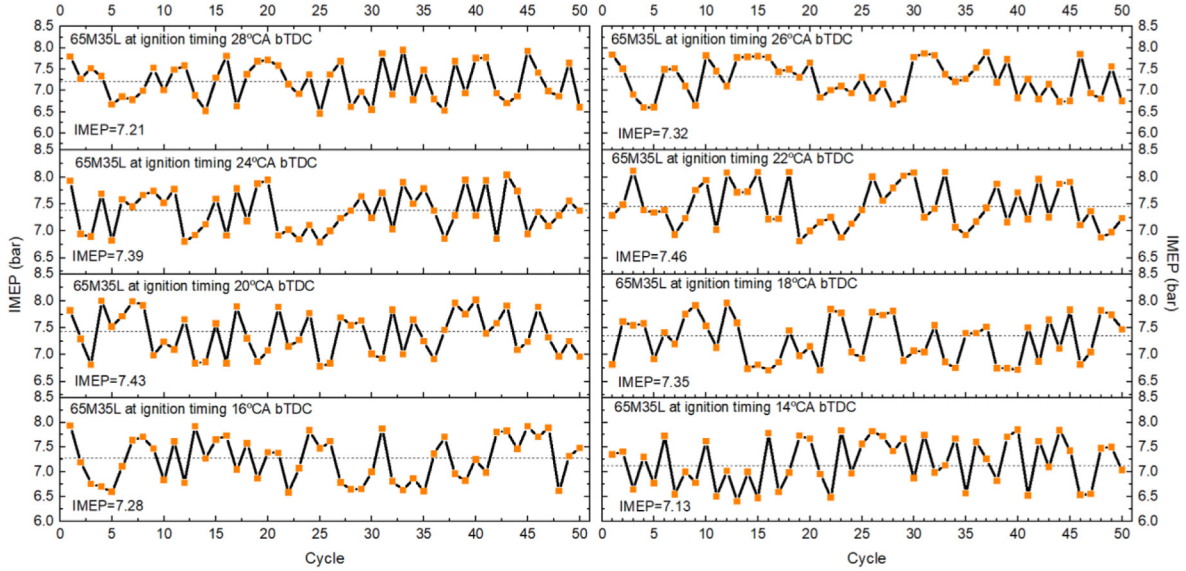

Figure 9. Cyclic variations of 65M35L.

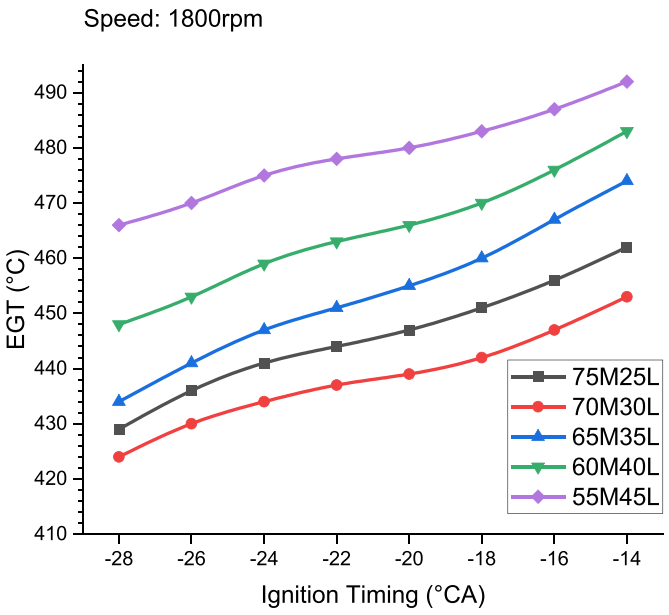

Figure 10. EGT variations with ignition timing at various Autogas fractions.

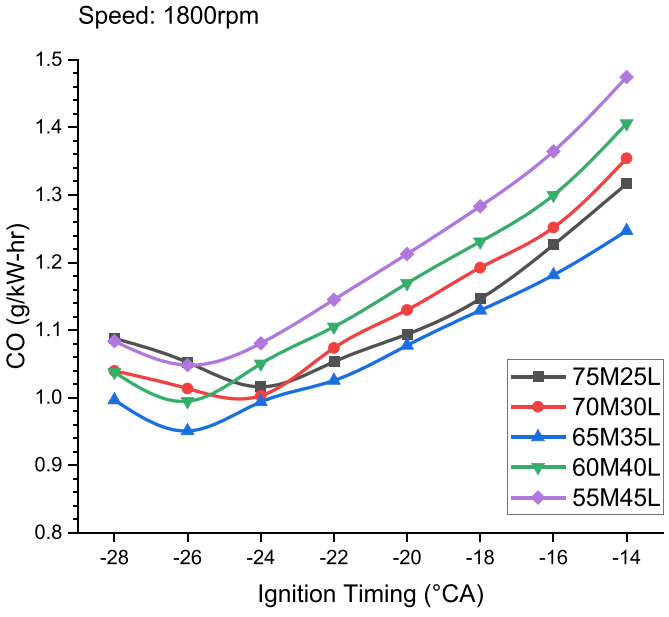

Figure 11. CO variations with ignition timing at various Autogas fractions.

3.7.2. HC emissions

HC emissions also follow the nearly same pattern as CO emissions; Figure 12 depicts it. It reduces with increasing methanol due to enhanced flame speed and quenching limit, reaching close to the cylinder and assuring complete combustion. Also, higher Autogas not only reduces the flame velocity of the mixture and increases the extent of stratification, creating heterogeneity near the spark plug. Therefore, CA10 elongates, which pushes a significant part of combustion to expansion stroke, increasing the probability of incomplete combustion and HC emissions. A 3.97% drop at 28°CA bTDC for 60M40L from 55M45L is observed, increasing to 6.04% for 65M45L. Increasing methanol above 65% allows latent heat factor to dominate, leading to improper combustion; hence, a slight increase for 70M30L from 65M35L is noticed. It is 4.29% greater than 55M45L at 28°CA bTDC, while for 75M25L, the HC emissions are 6.83% higher than 55M45L. While an ignition retard relives the gap between methanol-rich and Autogas-rich fuel, at 14°CA bTDC, there are

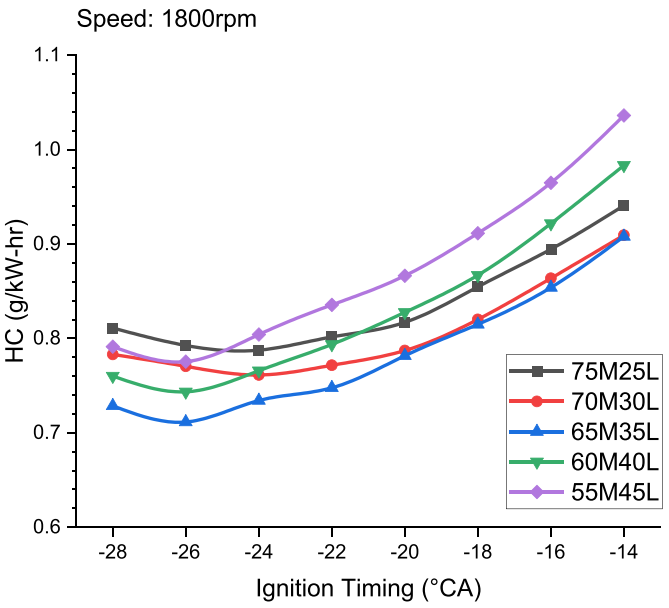

Figure 12. HC variations with ignition timing at various Autogas fractions.

7.7% fewer HC emissions for 75M25L than 55M45L. However, this benefit is insignificant after slight retard; at 75M25L, a 2.23% drop is noticed at 26°CA bTDC, which reduces to 0.62% at 24°CA bTDC. Retarding after 24°CA bTDC increases CO emissions due to shifting a large portion of combustion in the expansion stroke.

3.7.3. NO_x emissions

The specific NO_x emissions are directly linked to BP and depend mainly on T_{max} and λ. The NO_x emissions increase for 65M35L from 55M45L by 4.11% due to the increment of methanol at 28°CA bTDC; since methanol improves combustion, T_{max} rises more than BP (can be traced from BTE). Hence, volumetric NO_x rise dominates BP. However, increasing methanol further improves at 28°CA bTDC deteriorates combustion, T_{max} drops, and hence, NO_x drops. The drop rate intensifies with methanol strength, as, for 65M35L, it is 5.59%, and for 75M25L, it increases to 6.15% (Figure 13). In addition, at advanced ignition (28 (Figure 13)), Autogas combustion improves as slow-burning velocity stabilizes flame at the end of compression, increasing P_{max} and T_{max}. As a result, NO_x increases. However, retarding ignition for such fuel elongated

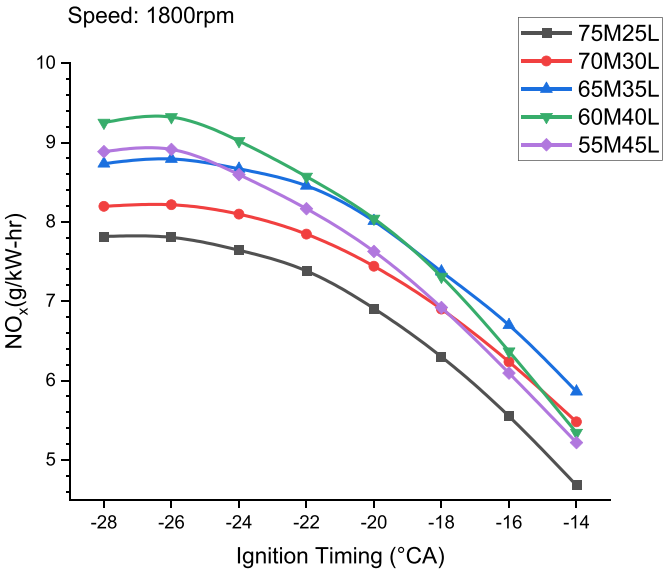

Figure 13. NO_x variations with ignition timing at various Autogas fractions.

combustion, T_{max} drops, leading to low NO_x, as an average 9.4%/2°CA reduction is noticed.

On the other hand, a methanol-rich fuel observes better combustion at retarded ignition and an increase in η_{vol}, leading to a large amount of oxygen at elevated T_{max}. Hence, NO_x increases for initial ignition retard. For 65M35L, a 1.1% increase is noticed by retarding ignition to 26°CA bTDC. However, increasing methanol above 65%, the MGT drops; hence, T_{max} drops could lead to NO_x drop, but a reduction in BTE leads to lower BP. Hence, NO_x increases slightly. Retarding ignition after 26°CA bTDC witnesses a rapid drop in T_{max}, while BTE drops gradually, significantly reducing NO_x emissions. There is an average 8.2% drop/2°CA ignition retard noticed.

4. Conclusion

The experimental study of Methanol/Autogas fuelled SI engine at variable ignition timing is performed on different mixture ratios under wide-open throttle (WOT) condition at 1800 rpm. The results are discussed in brief in the previous section with probable cause. Here, the outcomes are summarised and concluded as follows;

1. The ignition timing plays an important role in determining the combustion behavior and quality of the fuel; BTE improves with a slightly retarded ignition for the methanol-rich fuel. The ignition timing corresponds to peak BTE retards from 24°CA bTDC for 55M45L to 24°CA bTDC for 75M25L.
2. Methanol strength of the fuel significantly impacts combustion; it improves CA10 and CA10–90 to a minimum and then, reducing MGT due to increased latent heat, implicates a negative effect. Though an ignition retard, improves CA10, CA10–90 first improves and then deteriorates due to shifting in expansion stroke away from TDC.
3. P_{max} also improves by methanol up to 65M35L; however, peak advances till 70M30L. A further increase of methanol faces latent drawbacks, resulting in longer combustion and a retarded P_{max}. The ignition retard also shifts P_{max} away from TDC and reduces it due to the expansion cooling of the charge. T_{max} follows a similar pattern to P_{max}.
4. CO and HC emissions are reduced by methanol up to 65M35L due to improved combustion, which worsens after it. The ignition retard elongates combustion duration, and hence CO and HC emissions increase.
5. The NO_x emissions first increase with methanol up to 60M40L due to an increase in T_{max} and then drops slightly. For higher methanol, a significant drop in NO_x is noticed. However, ignition timing effectively reduces NO_x; as the combustion elongates, T_{max} reduces, which has a parallel impact on NO_x.
6. Methanol is observed to be better than Autogas up to a specific strength. The overall CO and HC emissions are pretty low due to the reduction in net carbon supply. The NO_x emissions are also lower than Autogas-rich duel. Hence, a more significant fraction could also be preferred neglecting the small impact on performance.

Declarations

Author contribution statement

Jayashish Kumar Pandey: Conceived and designed the experiments; Performed the experiments; Analyzed and interpreted the data; Contributed reagents, materials, analysis tools or data; Wrote the paper.

Dinesh M. H: Performed the experiments; Contributed reagents, materials, analysis tools or data.

Kumar G.N: Conceived and designed the experiment.

Funding statement

This research did not receive any specific grant from funding agencies in the public, commercial, or not-for-profit sectors.

Data availability statement

The authors do not have permission to share data.

Declaration of interest's statement

The authors declare no conflict of interest.

Additional information

No additional information is available for this paper.

References

[1] World LPG Association (WLPGA), Incentive policies, WLPGA Rep (2020).
[2] Gone E, Oral F. An Alternative Fuel for Internal Combustion Engines: Wood n.d.: 17–22.
[3] L. Raslavičius, A. Keršys, S. Mockus, N. Keršiene, M. Starevičius, Liquefied petroleum gas (LPG) as a medium-term option in the transition to sustainable fuels and transport, Renew. Sustain. Energy Rev. 32 (2014) 513–525.
[4] M.S. Bhatia, S.K. Jakhar, The effect of environmental regulations, top management commitment, and organizational learning on green product innovation: evidence from automobile industry, Bus. Strat. Environ. (2021) 1–12.
[5] M. Mrozik, A. Merkisz-guranowska, Environmental Assessment of the Vehicle Operation Process, 2021.
[6] M. Pichler, N. Krenmayr, E. Schneider, U. Brand, EU industrial policy: between modernization and transformation of the automotive industry, Environ. Innov. Soc. Transit. 38 (2021) 140–152.
[7] Y. Duan, T. Ji, Y. Lu, S. Wang, Environmental regulations and international trade: a quantitative economic analysis of world pollution emissions, J. Publ. Econ. 203 (2021), 104521.
[8] A.P. Singh, A. Pal, N.K. Gupta, A.K. Agarwal, Particulate emissions from laser ignited and spark ignited hydrogen-fueled engines, Int. J. Hydrogen Energy 42 (2017) 15956–15965.
[9] X. Zhen, Methanol as an Internal Combustion on Engine Fuel, Elsevier B.V., 2018.
[10] S.S. Araya, V. Liso, X. Cui, N. Li, J. Zhu, S.L. Sahlin, et al., A review of the methanol economy: the fuel cell route, Energies 13 (2020).
[11] C.J. Yang, R.B. Jackson, China's growing methanol economy and its implications for energy and the environment, Energy Policy 41 (2012) 878–884.
[12] V.K. Saraswat, R. Bansal, India' s Leapfrog to Methanol Economy, 2017, p. 10.
[13] Q.H. Hassan, G. Shaker Abdul Ridha, K.A.H. Hafedh, H.A. Alalwan, The impact of Methanol-Diesel compound on the performance of a Four-Stroke CI engine, Mater. Today Proc. 42 (2021) 1993–1999.
[14] S. Verhelst, J.W. Turner, L. Sileghem, J. Vancoillie, Methanol as a fuel for internal combustion engines, Prog. Energy Combust. Sci. 70 (2019) 43–88.
[15] Z. Tian, Y. Wang, X. Zhen, Z. Liu, The effect of methanol production and application in internal combustion engines on emissions in the context of carbon neutrality: a review, Fuel 320 (2022), 123902.
[16] B.S. Nathan Prasad, G.N. Kumar, Influence of ignition timing on performance and emission characteristics of an SI engine fueled with equi-volume blend of methanol and gasoline, Energy Sources art A Recover Util. Environ. Eff. (2019) 1–15.
[17] P.C. Mishra, A. Gupta, A. Kumar, A. Bose, Methanol and petrol blended alternate fuel for future sustainable engine: a performance and emission analysis, Meas. J. Int. Meas. Confed. 155 (2020), 107519.
[18] L. Wang, Z. Chen, T. Zhang, K. Zeng, Effect of excess air/fuel ratio and methanol addition on the performance, emissions, and combustion characteristics of a natural gas/methanol dual-fuel engine, Fuel 255 (2019), 115799.
[19] A. Elfasakhany, Performance and emissions of spark-ignition engine using ethanol–methanol–gasoline, n-butanol–iso-butanol–gasoline and iso-butanol–ethanol-gasoline blends: a comparative study, Eng. Sci. Technol. Int. J. 19 (2016) 2053–2059.
[20] A. Elfasakhany, A.F. Mahrous, Performance and emissions assessment of n-butanol–methanol–gasoline blends as a fuel in spark-ignition engines, Alex. Eng. J. (2016).
[21] M.B. Çelik, B. Özdalyan, F. Alkan, The use of pure methanol as fuel at high compression ratio in a single cylinder gasoline engine, Fuel 90 (2011) 1591–1598.
[22] Z. Li, C. Gong, X. Qu, F. Liu, J. Sun, K. Wang, et al., Critical firing and misfiring boundary in a spark ignition methanol engine during cold start based on single cycle fuel injection, Energy 89 (2015) 236–243.
[23] M. Abu-Zaid, O. Badran, J. Yamin, Effect of methanol addition on the performance of spark ignition engines, Energy Fuel. 18 (2004) 312–315.
[24] A. Bilgin, I. Sezer, Effects of methanol addition to gasoline on the performance and fuel cost of a spark ignition engine, Energy Fuel. 22 (2008) 2782–2788.
[25] C. Gong, F. Wei, X. Si, F. Liu, Effects of injection timing of methanol and LPG proportion on cold start characteristics of SI methanol engine with LPG enriched port injection under cycle-by-cycle control, Energy 144 (2018) 54–60.
[26] The Effect of Compression Ratio on the Performance, Emissions and Combustion of an SI (Spark Ignition) Engine Fueled with Pure Ethanol, Methanol and Unleaded Gasoline n.d..

[27] J.K. Pandey, G.N. Kumar, Effect of variable compression ratio and equivalence ratio on performance, combustion and emission of hydrogen port injection SI engine, Energy 239 (2022), 122468.
[28] M.H. Dinesh, J.K. Pandey, G.N. Kumar, Study of performance , combustion , and NO x emission behavior of an SI engine fuelled with ammonia/hydrogen blends at various compression ratio, Int. J. Hydrogen Energy (2022).
[29] B.S. Nathan Prasad, J.K. Pandey, G.N. Kumar, Impact of changing compression ratio on engine characteristics of an SI engine fueled with equi-volume blend of methanol and gasoline, Energy 191 (2020), 116605.
[30] Effect of Compression Ratio and Hydrogen Addition on Part Throttle Performance of a LPG Fuelled Lean Burn Spark Ignition Engine n.d..
[31] H. Chen, J. He, Z. Chen, L. Geng, A comparative study of combustion and emission characteristics of dual-fuel engine fueled with diesel/methanol and diesel–polyoxymethylene dimethyl ether blend/methanol, Process Saf. Environ. Protect. 147 (2021) 714–722.
[32] M.H. Dinesh, J.K. Pandey, G.N. Kumar, Effect of parallel LPG fuelling in a methanol fuelled SI engine under variable compression ratio, Energy 239 (2022), 122134.
[33] S. Somasundaram, T. Mohanraj, S. Pasupathy Raju, Effect of methanol additive with LPG in three cylinder four stroke S.I Engine, Appl. Mech. Mater. 592–594 (2014) 1503–1509.
[34] B. Patil, V. Nayak, M. Padmanabha, Emission and performance enhancement of multi-cylinder SI engine fuelled with LPG and vaporized water methanol induction, SAE Tech. Pap. (2014), 2014-Octob.
[35] C.M. Gong, J. Li, J.K. Li, W.X. Li, Q. Gao, X.J. Liu, Effects of ambient temperature on firing behavior and unregulated emissions of spark-ignition methanol and liquefied petroleum gas/methanol engines during cold start, Fuel 90 (2011) 19–25.
[36] C. Gong, Z. Liu, H. Su, Y. Chen, J. Li, F. Liu, Effect of injection strategy on cold start firing, combustion and emissions of a LPG/methanol dual-fuel spark-ignition engine, Energy 178 (2019) 126–133.
[37] M. Akif Ceviz, A.K. Sen, A.K. Küleri, I. Volkan Öner, Engine performance, exhaust emissions, and cyclic variations in a lean-burn SI engine fueled by gasoline-hydrogen blends, Appl. Therm. Eng. 36 (2012) 314–324.
[38] A. Javaheri, V. Esfahanian, A. Salavati-Zadeh, M. Darzi, Energetic and exergetic analyses of a variable compression ratio spark ignition gas engine, Energy Convers. Manage. 88 (2014) 739–748.
[39] I. Priyadarsini, M.V.S.M. Krishna, E.N. Devi, Study of Impact of Spark Timing and Compression Ratio on Performance of SI Engine, 2015, pp. 29–32.
[40] C. Gong, Z. Zhang, J. Sun, Y. Chen, F. Liu, Computational study of nozzle spray-line distribution effects on stratified mixture formation, combustion and emissions of a high compression ratio DISI methanol engine under lean-burn condition, Energy 205 (2020), 118080.
[41] A.A. Abdel-Rahman, M.M. Osman, Experimental investigation on varying the compression ratio of SI engine working under different ethanol-gasoline fuel blends, Int. J. Energy Res. 21 (1997) 31–40.
[42] J. Zheng, Z. Huang, J. Wang, B. Wang, D. Ning, Y. Zhang, Effect of compression ratio on cycle-by-cycle variations in a natural gas direct injection engine, Energy Fuel. 23 (2009) 5357–5366.
[43] S. Binjuwair, A. Alkudsi, The effects of varying spark timing on the performance and emission characteristics of a gasoline engine: a study on Saudi Arabian RON91 and RON95, Fuel 180 (2016) 558–564.
[44] J.K. Pandey, G.N. Kumar, Effects of hydrogen assisted combustion of EBNOL IN SI engines under variable compression ratio and ignition timing, Energy 246 (2022), 123364.
[45] J.K. Pandey, K.G. Narayanappa, Consequences of ignition timing on a hydrogen-fueled engine at various equivalence ratios, Energy Sources A Recover Util. Environ. Eff. 44 (2022) 6556–6567.
[46] J. Gao, G. Tian, C. Ma, L. Huang, S. Xing, Explorations of the impacts on a hydrogen-fuelled opposed rotary piston engine performance by ignition timing under part load conditions, Int. J. Hydrogen Energy 46 (2021), 11994–2008.
[47] Q. Tang, P. Jiang, C. Peng, H. Chang, Z. Zhao, Comparison and analysis of the effects of spark timing and lambda on a high-speed spark ignition engine fuelled with n-butanol/gasoline blends, Fuel 287 (2021), 119505.
[48] R.K. Prasad, N. Mustafi, A.K. Agarwal, Effect of spark timing on laser ignition and spark ignition modes in a hydrogen-enriched compressed natural gas fuelled engine, Fuel 276 (2020), 118071.
[49] S.K. Hotta, N. Sahoo, K. Mohanty, V. Kulkarni, Ignition timing and compression ratio as effective means for the improvement in the operating characteristics of a biogas fueled spark ignition engine, Renew. Energy 150 (2020) 854–867.
[50] J.K. Pandey, D. MH, K. GN, Consequences of varying compression ratio and ignition timing on engine fueled with E-MEBANOL, Int. J. Engine Res. (2022).
[51] Energy-Economic Evaluation of a New Drying System Boosted by Ranque-Hilsch Vortex Tube n.d..
[52] M.H. Dinesh, G.N. Kumar, Energy conversion and management: X effects of compression and mixing ratio on NH3/H2 fueled Si engine performance, combustion stability, and emission, Energy Convers. Manage. X 15 (2022), 100269.
[53] E. Pipitone, S. Beccari, Performances and emissions improvement of an S.I. engine fuelled by LPG/gasoline mixtures, SAE Tech Pap (2010).
[54] H. Bayraktar, O. Durgun, Investigating the effects of LPG on spark ignition engine combustion and performance, Energy Convers. Manage. 46 (2005) 2317–2333.
[55] M. Baloo, B.M. Dariani, M. Akhlaghi, M. Aghamirsalim, Effects of pressure and temperature on laminar burning velocity and flame instability of iso-octane/methane fuel blend, Fuel 170 (2016) 235–244.
[56] Kawahara N, Roy MK, Fujitani T, Tomita E. Effect of Spark Timing on Combustion Characteristics in a Direct-Injection Hydrogen Engine n.d.:1–2.